

Spectroscopic identification of histamine using metalloporphyrins and their electrochemical characterization

ANA-MARIA IORDACHE^a, STEFAN-MARIAN IORDACHE^{a,*}, ROXANA BOHILTEA^{b,*}, VALENTIN BARNA^c, CONSTANTIN RIZEA^d, ALEXANDRA MAZLUM^d, VALENTINA CAPATINA^e, CRISTIANA EUGENIA ANA GRIGORESCU^a

^aNational Institute of R&D in Optoelectronics, INOE 2000, 409 Atomistilor St., 077125, Magurele, Jud. Ilfov, Romania^{2,3}

^b"Carol Davila" University of Medicine and Pharmacy Bucharest, 37 Dionisie Lupu St., 020021, Bucharest, Romania

^cUniversity of Bucharest, Faculty of Physics, 405 Atomistilor St., P.O. Box MG-38, 077125, Magurele, Romania

^dRoxy Veterinary S.R.L., 52A Unirii St., Magurele, 077125, Romania

^eMGM Star Construct S.R.L., 7B Pancota St., Bucharest, Romania

Due to their π -extended conjugated electronic system, porphyrins are excellent candidates for sophisticated energy transfer devices, including sensors. Their versatile optical and photochemical behaviour have eased the functionalization of porphyrins and their derivatives with different molecules, antenna-like sensors capable of identifying down to ppb levels of analytes. In this study, we present the spectroscopic identification of histamine using Zn-porphyrin and the electrochemical behaviour of Co- and Mn-porphyrins immobilized by dropcasting onto carbon-based screen-printed electrodes (SPEs). The cyclic voltammetry studies performed on the three metalloporphyrins showed different behaviours towards histamine detection, particularly in the presence of trichloroacetic acid, used as reaction mediator.

(Received November 2, 2021; accepted November 24, 2021)

Keywords: Raman spectroscopy, UV-Vis spectroscopy, Cyclic voltammetry, Metalloporphyrin, Histamine

1. Introduction

Recent concerns about climate change, fossil fuels depletion and waste management have led to the development of green chemistry as frontier field of continuously evolving interdisciplinary science. Natural products (including bio-waste) [1], [2] have been used to synthesize cutting-edge bio-nanoarchitectures for various fields, such as: energy storage devices [3], [4] low-toxicity nanoparticles [5], optical limiting devices [6], [7], antimicrobial therapy [8] and sensors [9], [10], [11].

Porphyrins are colored biological molecules, which mimic the active site of many important enzymes and are used in many analytical applications [12]. One of the most important is the detection of histamine [13], [14], which is a biogenic amine commonly used as indicator of food spoilage [15]. A fresh food product should have a concentration of histamine around 10 mg/kg [15], since a level between 11–40 mg/kg of histamine can produce minor poisoning in humans [16]. Product alteration is observed for levels of histamine above 30 mg/kg, whereas levels above 100 mg/kg show decomposition and produce severe poisoning [13], [15], [16].

In this study, we selected three metalloporphyrins and investigated their spectroscopic and electrochemical behavior in the presence of different concentrations of histamine. To facilitate charge transfer between histamine and metalloporphyrin, we used trichloroacetic acid as reaction mediator.

2. Experimental

2.1. Materials

We selected three metalloporphyrin, purchased as powders from Sigma-Aldrich (Merck KGaA, Darmstadt, Germany): (1) Mn-porphyrin: (5,10,15,20-Tetraphenyl-21H,23H-porphine manganese(III) chloride); (2) Zn-porphyrin: Zinc 5,10,15,20-tetra(4-pyridyl)-21H,23H-porphine, and (3) Co-porphyrin: 5,10,15,20-Tetrakis(4-methoxyphenyl)-21H,23H-porphine cobalt(II). The metalloporphyrins were then dispersed in chloroform (99%, Merck) at a concentration of 5mg/mL.

Histamine (99%, Sigma Aldrich) and trichloroacetic acid (TCA 99%, Merck) were used as received without other purification. We also employed distilled water and phosphate buffer solution (PBS), which was prepared daily from 20.2 g monosodium phosphate ($\text{NaH}_2\text{PO}_4 \cdot 2\text{H}_2\text{O}$) and 3.4 g disodium phosphate ($\text{Na}_2\text{HPO}_4 \cdot 12\text{H}_2\text{O}$), having the pH=7.4.

The suspensions of metalloporphyrins in chloroform samples were deposited onto screen-printed electrodes (SPE-C-110 from Metrohm DropSens), composed of three planar electrodes on ceramic substrate. The working (WE) and auxiliary (AUX) electrodes were made of carbon and the pseudoreference electrode was made of silver. WE was a thin disc of carbon with an area of 0.125 cm². The AUX and the reference electrode were screen-printed in a circle surrounding the WE at a distance of 1 mm.

2.2. Functionalization of the screen printed electrode

Functionalization of the SPEs was performed by dropcasting 5 μl of metalloporphyrin in chloroform dispersion on the gold working electrode surface, in single batches of 1 μl . Afterwards, the solution was left to dry at 50°C under IR light.

2.3. Characterization methods

Spectroscopic studies were performed on a Raman spectrometer (Jasco NRS 3100, 532 nm) and on a UV-Vis spectrophotometer (UV/VIS/NIR Jasco V570). The UV-Vis solutions were prepared by mixing 1.5 mL metalloporphyrins in chlorophorm with 1.5 mL TCA 0.3% solution and 100 μL solution of 100 ppm histamine. Cyclic voltammetry was performed on a Voltalab 40 system (Radiometer Analytical) adapted for SPEs. The current density variation was recorded for a potential sweep from -750mV to +1000 mV. For each experiment 100 μl solution was dispersed on the modified SPE in order to cover with a thin film the WE, AUX and reference electrodes.

3. Results

3.1. Raman spectroscopy

The Raman spectra show the peaks which are common to the metalloporphyrins sharing a ring of four pyrrole functional groups, and individual traits. The common peaks correspond to the symmetric deformation/rotation mode (δ_{sym}) of the pyrrole frame (at 1248 cm^{-1} for Zn, at 1265 cm^{-1} for Mn and at 1255 cm^{-1} for Co) and the symmetric stretching mode (ν_{sym}) for the C-H bond (presented at 1058 cm^{-1} for Co and Mn and at 1026 cm^{-1} for Zn) [13]. Zn-porphyrin shows a peak at 380 cm^{-1} which is attributed to the Zn-C bond.

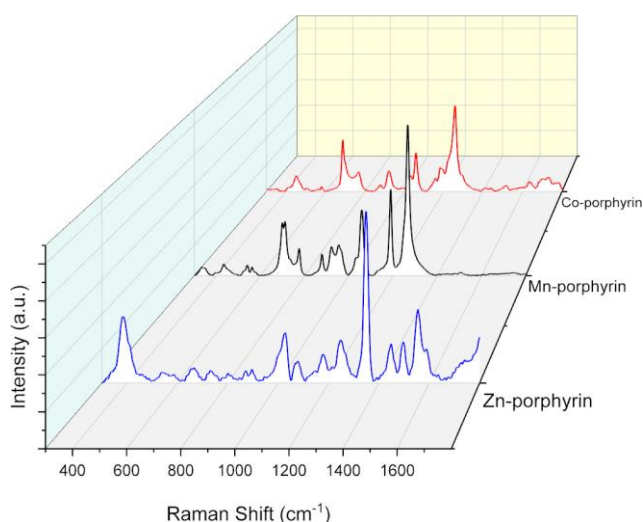


Fig. 1. Raman spectra for the three metalloporphyrins (color online)

3.2. UV-Vis spectrophotometric detection of Histamine

The UV-Vis spectrum of histamine is presented in Fig. 2 and it shows two intense peaks at 228 nm and at 435 nm. Compared to the spectrum of the Zn-porphyrin +TCA+histamine system, the two intense peaks are maintained, but transposed at higher wavelengths due to red shifting.

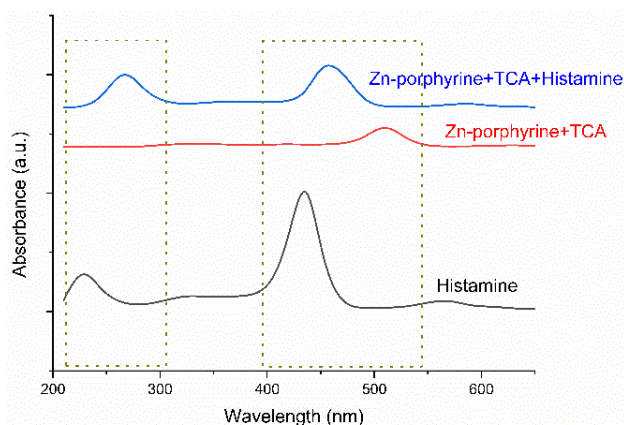


Fig. 2. UV-Vis identification of histamine by Zn-porphyrin (color online)

When overlaying the spectrum of Zn-porphyrin with TCA, the peak at 451 nm (in the Zn-porphyrin+TCA+histamine) is composed from the absorption peaks of histamine and TCA solution. This is produced by the formation of a complex molecular compound between histamine and TCA [13]. TCA is commonly used in HPLC (high performance liquid chromatography) for sample pretreatment to derivative biogenic amines [17], [18] because it acts as an electron donor. The electronic configuration of the metallic ion in the centre of the porphyrin guides the sensitivity of the determination. For Zn (II), the electronic configuration shows a fully occupied d subshell of the 3rd energy level (3d¹⁰), whereas for the Co (II) it is only half occupied (3d⁵) and for Mn (III) it is occupied with only two electrons (3d²). It is in our opinion that when the intermediary compound TCA-histamine reaches the Zn-porphyrin, the Zn ion cannot capture the electrons released by the molecular complex due to its fully occupied state. But the Co-porphyrin and Mn-porphyrin can capture those electrons, which are thus transferred to the metallic ion and the intermediary complex is broken into its constituents: histamine and TCA. This is why the Co-porphyrin and Mn-porphyrin cannot discriminate between TCA and histamine.

3.3. Histamine detection via cyclic voltammetry

Fig. 3 presents the results of the cyclic voltammetry for Co-porphyrin in different concentrations of histamine and 0.3% TCA. The curve (inset Fig. 3) shows a quasi-reversible reaction, with a large double layer. The oxidation potential for the couple histamine-TCA appears as a peak

around +50mV and a broad plateau between +150-200 mV. An increase of the concentration of histamine produces a steady rise in the current density of the oxidation reaction. However, for 5 ppm histamine the current density is superior compared with the following concentrations. This high current density is maintained through all five measurements and is not an error of the equipment and/or of the sample preparation. We could not find a satisfactory explanation for this behaviour although we believe that the detection mechanism follows two different processes for concentrations < 5 ppm and > 10 ppm.

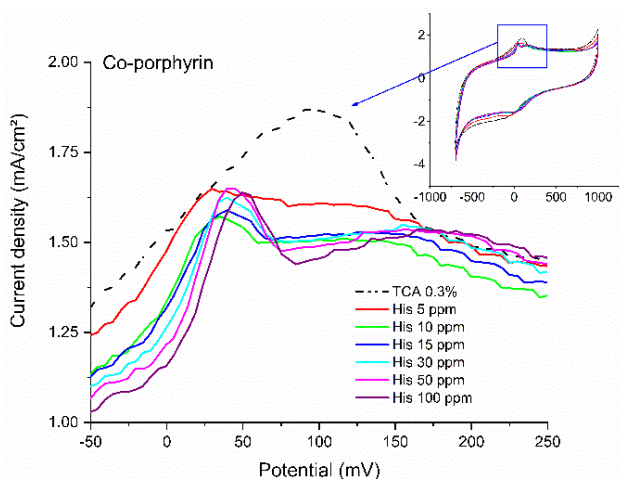


Fig. 3. Cyclic voltammetry for the Co-porphyrin SPE for different concentrations of histamine (color online)

Mn-porphyrin exhibits an increase of the peak intensity at +50 mV as well as a small increase (+350 $\mu\text{A}/\text{cm}^2$ for the 100 ppm His curve) of the current density for the broad plateau (Figure 4). This behaviour is explained by the different oxidation state of the metallic ion at the porphyrin coordination site: Co has an oxidation state of (II) and requires less potential to be reduced (and re-oxidized) to the same oxidation state compared to Mn that has an oxidation state of (III) and requires two steps – an initial oxidation to (II) and a second oxidation (from II to III).

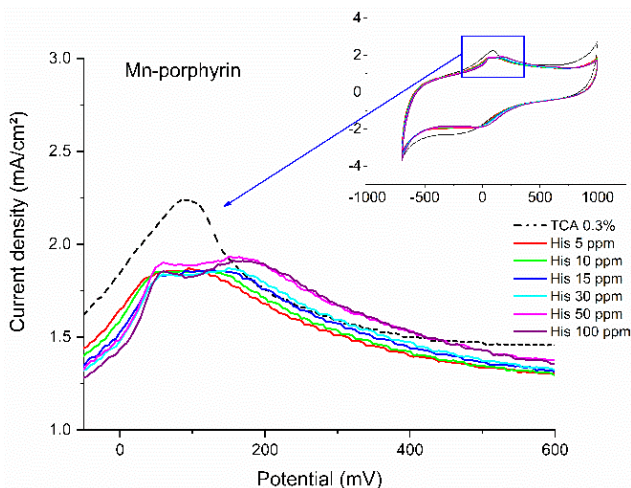


Fig. 4. Cyclic voltammetry for the Mn-porphyrin SPE in different concentrations of histamine (color online)

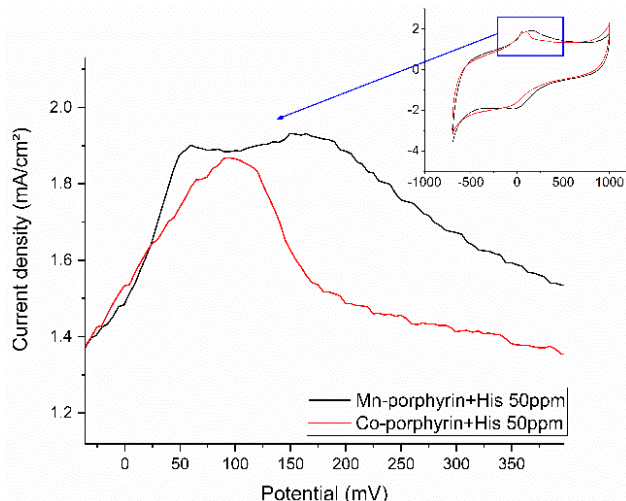


Fig. 5. Cyclic voltammetry for the two metalloporphyrins in 0.3% TCA and 50 ppm histamine (color online)

In Fig. 5 we demonstrate a comparison of the characteristics for Co and Mn-porphyrins at 50 ppm histamine and 0.3% TCA. This graph reveals the energy drawn from the circuit by the metallic ions to undergo oxidation and also supports the previous results shown in Figs. 4 and 5.

Zn-porphyrin in combination with TCA 0.3% reacted with the plastic cover of the screen printed sensors and could not be tested in good conditions.

4. Conclusions

Three metalloporphyrins (Co, Zn and Mn) were studied in order to assess their behaviour towards histamine detection. Zn-porphyrin was a good choice as optic sensor for the detection of histamine in liquid samples. However, the electrochemical behavior could not be assessed since even in 0.3% TCA, Zn-porphyrin reacted with the plastic cover of the SPEs causing their exfoliation. For the Mn- and Co-porphyrins, initial trials confirmed the TCA as optimal mediator and the 0.3% concentration maintained the integrity of the SPEs. The two metalloporphyrins react differently to the histamine, depending on the oxidation state of the coordinated metal ion: Co has an oxidation state of (II) and the electron transfer occurs at +50 mV, followed by a low intensity broad plateau above +150mV, whereas Mn has a slow oxidation towards Mn(II) followed by a quick and pronounced oxidation to Mn(III).

Acknowledgements

This work was supported by a grant of the Romanian Ministry of Education and Research, CNCS - UEFISCDI, project number PN-III-P1-1.1-PD-2019-1134 (Ctr. No. PD87/2020), PN-III-P2-2.1-PED-2019-2551 (Ctr. No. 393PED/2020), Program MANUNET-UEFISCDI (Ctr. MNET 213/2020), CORE Programme, Ctr. 18/N/2019 within PNCDI III.

References

- [1] M. E. Barbinta-Patrascu, *Optoelectron. Adv. Mat.* **13**(9-10), 546 (2019).
- [2] M. E. Barbinta-Patrascu, C. Ungureanu, D. Besliu, A. Lazea-Stoyanova, L. Iosif, *Optoelectron. Adv. Mat.* **14**(9-10), 459 (2020).
- [3] L. Liangshuo, Q. Lin, L. Xinyu, D. Ming, F. Xin, *Optoelectron. Adv. Mat.* **14**(11-12), 548 (2020).
- [4] M. Joseph, S. Haridas, *Int. J. Hydrog.* **45**, 11954 (2020).
- [5] Y. Long, J. Hao, Y. Liu, W. Yang, *Optoelectron. Adv. Mat.* **14**(11-12), 556 (2020).
- [6] A. Wang, L. Cheng, W. Zhao, W. Zhu, D. Shang, *Dyes Pigm.* **161**, 155 (2019).
- [7] A. Wang, X. Du, Y. Yin, X. Shen, L. Cheng, W. Zhu, D. Shang, *Diam. Relat. Mater.* **106**, 107838 (2020).
- [8] U. Sah, K. Sharma, N. Chaudhri, M. Sankar, P. Gopinath, *Colloids Surf. B Colloid Surface B* **162**, 108 (2018).
- [9] L. Lvova, M. Mastroianni, G. Pomarico, M. Santonico, G. Pennazza, C. D. Natale, R. Paolesse, A. D'Amico, *Sens. Actuators B Chem.* **170**, 163 (2012).
- [10] J.-S. Lee, D.-W. Jeong, Y. T. Byun, *Sens. Actuators B Chem.* **306**, 127518 (2020).
- [11] K. Prakash, M. Sankar, *Sens. Actuators B Chem.* **240**, 709 (2017).
- [12] D. Y. Seong, M.-S. Choi, Y.-J. Kim, *Eur. Polym. J.* **48**, 1988 (2012).
- [13] A.-M. Iordache, R. Cristescu, E. Fagadar-Cosma, A. C. Popescu, A. A. Ciucu, S. M. Iordache, A. Balan, C. Nichita, I. Stamatina, D. B. Chrisey, *C. R. Chim.* **21**(3-4), 270 (2018).
- [14] M. E. Bakkari, B. Fronton, R. Luguya, J.-M. Vincent, *J. Fluor. Chem.* **127**, 558 (2006).
- [15] C. Amorim, R. Souza, A. Araújo, M. Montenegro, V. Silva, *Food Chem.* **122**, 871 (2010).
- [16] I. Basozabal, A. Guerreiro, A. Gomez-Caballero, M. A. Goicolea, R. J. Barrio, *Biosens. Bioelectron.* **58**, 138 (2014).
- [17] H. Harmoko, R. E. Kartasmita, H. Munawar, A. Rakhmawati, B. Budiawan, *Journal of Food Composition and Analysis* **105**, 104256 (2022).
- [18] A. Önal, S. E. K. Tekkeli, C. Önal, *Food Chem.* **138**, 509 (2013).

*Corresponding author: stefan.iordache@inoe.ro;
r.bohiltea@yahoo.com